

Dynamics of intramolecular vibrational-energy redistribution (IVR).

III. Role of molecular rotations

Peter M. Felker^{a)} and Ahmed H. Zewail^{b)}

Arthur Amos Noyes Laboratory of Chemical Physics,^{c)} California Institute of Technology, Pasadena, California 91125

(Received 9 November 1984; accepted 17 December 1984)

Experimental results on jet-cooled anthracene pertaining to the role of rotations in IVR processes are presented. For theoretical comparison, we consider the effects of molecular rotational level structure on the beat-modulated decays that arise as manifestations of IVR. It is shown theoretically for anharmonic coupling that small differences in rotational constants between coupled vibrational states give rise to decays, the beat envelopes of which decay faster than the unmodulated portions of the decays. These envelope decay rates are shown to be rotational temperature dependent. The experimental results reveal behavior entirely consistent with the theoretical expectations. The results also show that although rotational effects are present in experimental decays, they are not so marked as to wash out the manifestations of vibrational coherence.

I. INTRODUCTION

In the theoretical treatment of vibrational quantum beats (paper I¹) and in the interpretations of experimental results²⁻⁶ pertaining to this phenomenon that have been reported on by this laboratory, little attention has been directed toward one molecular characteristic that might be expected to play a large role in influencing the observed consequences of vibrational coupling: the fact that each vibrational level is actually an entire manifold of rotational levels. In some sense, our neglect of this aspect of molecular level structure can be justified by the close correspondence between the theory constructed without its inclusion and experimental results.^{2-4,6} This argues that the observed results are, on the whole, manifestations of vibrational couplings which are weakly dependent on rotational level. On the other hand, we have reported⁵ some results which can only be interpreted by taking into account the rotational level structure. Moreover, a comprehensive description of vibrational quantum beats should come to terms with the manifestations that can arise from rotational effects on vibrational coupling. This is a particularly pertinent task being that it has been widely believed⁷ that such effects preclude the possibility of observing vibrational quantum beats in the fluorescence of large molecules, even molecules cooled by supersonic expansion; the number of populated ground state rotational levels and the variation in vibrational coupling with rotational level in the excited state are thought to be large enough that any coherence effects due to rovibration-rovibration coupling will be washed out. In actual fact, the number of superimposed incoherent excitations due to rotational level structure is large for large molecules (like anthracene), even at very low rotational temperatures (e.g., 2 K). It is clear, however, that vibrational quantum beats can be observed for such molecules. Therefore, it

must be that rotational effects on vibrational coupling need not be so marked as to render quantum beats unobservable. Yet, it may also be true that such effects are large enough to manifest themselves more subtly in beat-modulated decays.

Since the first observation² of phase-shifted quantum beats in anthracene, one characteristic has been noted which cannot be reconciled with theoretical predictions. While theory¹ predicts essentially equal decay rates for the amplitudes of the modulated and unmodulated portions of a given decay, it has been observed in general that the amplitude of the modulated portion of an experimental decay (i.e., the quantum beat envelope) decays faster than that of the unmodulated portion (i.e., the lifetime-type decay). Two aspects of this discrepancy point toward a rotational involvement in vibrational coupling. Firstly, the theory in question does not account for rotations, and it is plausible to attribute the errors in theoretical predictions to the neglect of such a factor. Secondly, and more significantly, an increased beat decay rate implies that the widths of the beat components in the frequency domain are greater than the width of the zero frequency component corresponding to the unmodulated exponential. An increased width is just what one would expect given vibrational couplings which are dependent on rotational level.

In an effort to establish a firmer link between quantum beat envelope decays and rotational influences we have performed a number of experiments and theoretical simulations. At the heart of both the experimental and theoretical approaches is the fact that if vibrational coupling is dependent on rotational level, then this will be manifested as a dependence of beat-modulated fluorescence decays on the rotational temperature of the sample. By varying this temperature and observing the changes in decays, one can assess the rotational influences on beats.

In this paper, we present experimental results which show that the decay rates of quantum beat envelopes of jet-cooled anthracene increase significantly as the rota-

^{a)} IBM Graduate Fellow.

^{b)} Camille and Henry Dreyfus Foundation Teacher-Scholar.

^{c)} Contribution No. 7118.

tional temperature of the sample increases. This behavior is found to be consistent with the results of theoretical simulations for which it is assumed that (1) vibrational levels are coupled by anharmonic coupling and (2) rotational effects on this coupling arise solely from the differences in rotational constants between coupled vibrational levels. The results lead us to conclude that rotational effects on vibrational coupling need not wash out the manifestations of vibrational coherence in large molecules, but may be subtly manifest in observed beat-modulated decays.

II. THEORETICAL SIMULATIONS

A. Outline of calculations

In this section the results of calculations designed to elucidate the effects which rotational temperature may have on vibrational quantum beats in anthracene will be presented. First, however, it is pertinent to outline these calculations and point out the various approximations inherent in them. A basic assumption involved in the computations is that any coherence effects due to the coherent excitation of rotational levels within the *same* vibrational state are negligible. This assumption, which can be justified on experimental and theoretical grounds,⁸ has the consequence of allowing one to calculate a fluorescence decay simply by summing the individual decays associated with individual rotational levels. In particular, if one adopts the definitions and nomenclature of the previous two papers,^{1,6} and considers the fluorescence intensity $I_\gamma(t)$ of a γ -type fluorescence band, then

$$I_\gamma(t) = \sum_{J=0}^{\infty} \sum_{K_a=-J}^J W(J, K_a, T) I_\gamma(J, K_a, t), \quad (2.1)$$

where J and K_a are the usual rotational quantum numbers of an approximate prolate symmetric top⁹ and refer to rotational levels in the manifold of the $|a\rangle$ (optically active) zero-order vibrational level, T is the rotational temperature of the sample, $W(J, K_a, T)$ is a weighting factor for each rovibrational level $|a, J, K_a\rangle$, and $I_\gamma(J, K_a, t)$ is the γ -type fluorescence decay which arises from the coupling of $|a, J, K_a\rangle$ with the rotational levels of the other zero-order vibrational states.

To calculate $I_\gamma(t)$ from Eq. (2.1) it is very useful to make several simplifying approximations. The first has already been mentioned; the molecule is treated as an approximate symmetric top. This allows one to calculate the rotational energy of a given rotational level $|J, K_a\rangle$ as⁹

$$E(J, K_a) = \frac{1}{2}(B + C)J(J + 1) + [A - \frac{1}{2}(B + C)]K_a^2, \quad (2.2)$$

where A , B , and C are the rotational constants of the molecule. A second useful approximation is the assumption that the thermal distribution of ground state rotational levels that exists prior to the excitation of the sample is projected into the excited state upon excitation. One then obtains the following expression⁹ for the weighting factor in Eq. (2.1):

$$W(J, K_a, T) = g_N(J, K_a)(2J + 1)\exp[-E(J, K_a)/k_B T], \quad (2.3)$$

where $g_N(J, K_a)$ is the nuclear spin statistical weight and k_B is Boltzmann's constant. A third approximation involves limiting the sum over J in Eq. (2.1). This is justified by the expectation that $W(J, K_a, T)$ will become small for high enough J, K_a . The calculations reported here for anthracene were made for $J \leq 30$. No significant qualitative deviations from the results of these calculations were noted when the J range was increased to $J = 60$ and beyond.

The factors $I_\gamma(J, K_a, t)$ in Eq. (2.1) represent the effects of rovibrational coupling in the decay. The form which these terms take depends wholly on the assumptions made concerning the coupling. Once these assumptions are made, $I_\gamma(J, K_a, t)$ can be calculated by first diagonalizing the rovibrational Hamiltonian for $|a, J, K_a\rangle$ and all the levels coupled to it, and then by using the eigenvalues obtained to get the modulation depths (magnitudes and phases) of the beat components.¹⁰

Knowing both $W(J, K_a, T)$ and $I_\gamma(J, K_a, t)$ for all pertinent rotational levels, $I_\gamma(t)$ can be calculated. The calculations of $I_\gamma(t)$ presented in this paper have been performed in such a way as to allow direct comparison with experimental decays. In particular, it is not actually the $I_\gamma(t)$ which are shown in the figures but convolutions of typical temporal response functions with $I_\gamma(t)$ [see Eq. (2.1) of paper II]. Also, the simulated decays have been calculated for one thousand discrete points in time to match the number of channels that were used for collecting experimental decays.

B. Rotational states in anthracene

Anthracene is an asymmetrical top characterized by rotational constants $\frac{1}{2}(B + C)$ and $A - \frac{1}{2}(B + C)$ that are equal to ~ 0.415 and 1.74 GHz,¹¹ respectively. The molecule has D_{2h} point group symmetry. Therefore, every group of four adjacent rotational levels, with the lowest energy level of a given group being either the 1st, 5th, ..., or $4m + 1$ st level in the manifold, has one and only one level corresponding to each of the four irreducible representations of the D_2 rotational subgroup—i.e., A , B_1 , B_2 , and B_3 .⁹ Rotational levels of different symmetry are, in general, characterized by different nuclear spin statistical weights [the $g_N(J, K_a)$ of Eq. (2.3)]. For the vibrationless level of the ground state of anthracene, the statistical weights were calculated following the procedure of Ref. 12 and were found to be 18, 15, 16, and 15 for the A , B_1 , B_2 , and B_3 rotational levels, respectively (the x axis was taken as the long in-plane axis and the z axis as the out-of-plane axis of the molecule). For the simulations which we present here, we ignore the small differences between the statistical weights and take them all to be equal. This approximation increases the ease of calculation. It is a reasonable approximation for two reasons. Firstly, the differences between weights are small ($\leq 20\%$). Secondly, even at the low rotational temperatures in the jet, a large number of anthracene rotational levels are

significantly populated, owing to the small rotational constants of the molecule. Therefore, the small effects due to the slightly different statistical weights will tend to be averaged over a large number of rotational levels. It is pertinent to note that in other cases involving smaller molecules (e.g., benzene)¹³ with larger rotational constants and more widely varying statistical weights, the weights must be explicitly taken into account to explain spectroscopic results. As for the observation of beats, population of these nuclear states leads to an inhomogeneous superposition of spectral lines, which as shown below does not lead to a smearing out of beats (as suggested by some⁷).

C. Vibrational coupling

In general, there are two types of interactions that might be expected to be prominent in the coupling of two or more vibrational states. These are anharmonic and Coriolis interactions. In this section we shall be concerned with rotational effects in anharmonic coupling. In Sec. V we will discuss experimental manifestations of anharmonic and Coriolis interactions.

The influence of symmetry on rotational couplings leading to radiationless transitions in molecules has been considered in detail elsewhere.¹⁴⁻¹⁶ Anharmonic coupling between zero-order rovibrational levels is characterized by two general features (see Fig. 1). Firstly, angular momentum selection rules and symmetry restrictions⁹ limit this type of coupling to rovibrational levels of $|a\rangle$, $|b\rangle$, $|c\rangle$, ... having the same J , K_a values. Thus, for a coupling between N vibrational states, one need only consider an $N \times N$ Hamiltonian matrix for each value of

J , K_a , the rows and columns of such a matrix being labeled by the zero-order states $|a, J, K_a\rangle$, $|b, J, K_a\rangle$, $|c, J, K_a\rangle$, ... Secondly, the off-diagonal elements of the Hamiltonian matrices do not change with rotational level⁹ (to first order). As a consequence of this, $I_\gamma(J, K_a, t)$ only depends on J , K_a through variations in the energy spacings of the zero-order levels; i.e., variations in the differences between diagonal elements of the Hamiltonian matrix. Such variations with rotational level can occur if some of the coupled vibrational states have different rotational constants, in which case the zero-order energy differences between states $|\gamma\rangle$ and $|\gamma'\rangle$ can be expressed as

$$E_{\gamma\gamma}(J, K_a) = E_{\gamma\gamma}(0, 0) + \Delta_{\gamma\gamma} \left(\frac{B+C}{2} \right) J(J+1) + \Delta_{\gamma\gamma} \left(A - \frac{B+C}{2} \right) K_a^2, \quad (2.4)$$

where $\Delta_{\gamma\gamma}(B+C)/2$ and $\Delta_{\gamma\gamma}[A - \frac{1}{2}(B+C)]$ represent the mismatches in rotational constants between $|\gamma\rangle$ and $|\gamma'\rangle$.

The perturbations which contribute to rotational constant mismatches between vibrational states are small ones.⁹ Thus, these mismatches are expected to be small fractions of the mean rotational constants. Being that data pertaining to the rotational constants of vibrational states of aromatics are hard to come by, an order of magnitude for the effect has been assumed after consideration of more readily available measurements of the changes in constants between *electronic* states.⁹ Such changes are on the order of several parts in a thousand. For the results presented herein it has been assumed that rotational mismatches between vibrational states are roughly one part in one thousand. For anthracene, this means that $\Delta_{\gamma\gamma}(B+C)/2 \sim 0.4$ MHz and $\Delta_{\gamma\gamma}[A - \frac{1}{2}(B+C)] \sim 1.7$ MHz. Actual values for mismatches for a given calculation were generated by a random number generator constrained to produce rotational constants within a set range.

Two-level coupling is conceptually the easiest case since there are only pairwise interactions up the rotational level structure of the coupled vibrational states (see Fig. 1). One expects the overall coupling between manifolds to give rise to a large number of different beat frequencies, each corresponding to the interaction of a pair of rovibrational levels, but all being fairly close to some average value. At finite rotational temperatures one expects that the superposition of all of these different fluorescence decays will result in a total fluorescence decay in which only one beat component appears to be present and in which the rate of decay of the beat envelope will be greater than the decay rate of the unmodulated portion of the transient. Moreover, this envelope decay rate should increase with increasing rotational temperature. In Fig. 2 we show calculated results of both *a*- and *b*-type decays for a model two-level system. For these calculations $E_{ab}(0, 0)$ of Eq. (2.4) and V_{ab} , the anharmonic coupling matrix element, have been chosen to be 2.24 and 1.0, respectively, to give typical values for both the beat frequencies (3 GHz) and the modulation depth (0.28) of

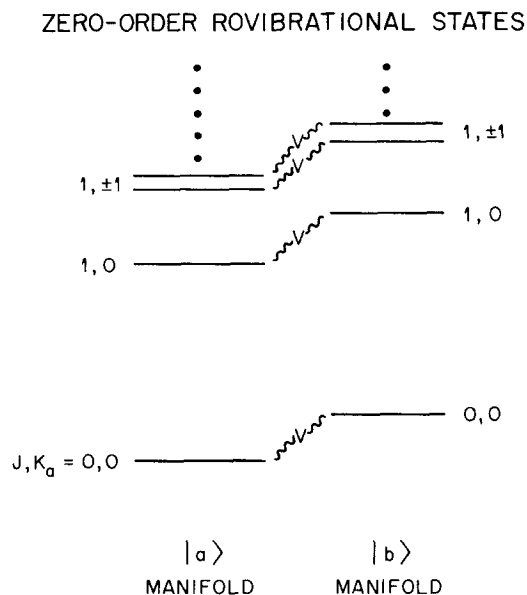


FIG. 1. Schematic diagram of the anharmonic coupling between the rotational levels of two zero-order vibrational states— $|a\rangle$ (left) and $|b\rangle$ (right). Only those rotational levels having the same rotational quantum numbers (J , K_a) are coupled. Moreover, the coupling matrix element V , is constant for each pair of coupled rovibrational states. Coupling can vary up the rotational manifold only through differences in energy spacings between coupled states. (Such differences are not shown in the figure.) Note that there has been no attempt to draw the spacings between levels to scale.

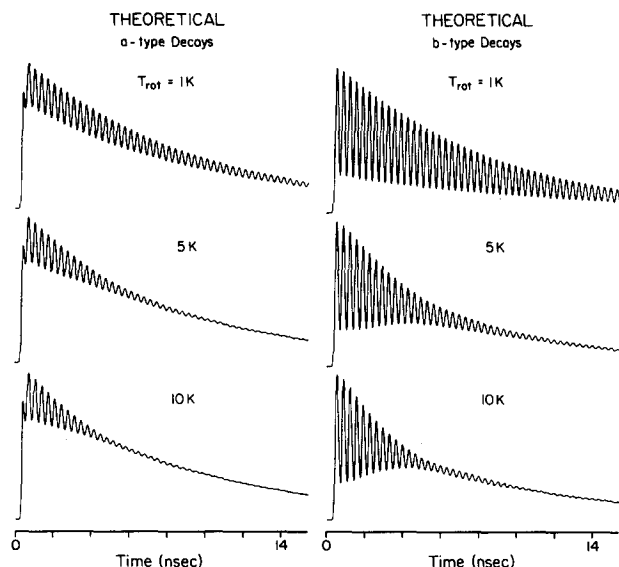


FIG. 2. Simulated decays as a function of rotational temperature for the a - and b -type decays of a coupled two level system. The lowest rotational states of the two zero-order levels were taken to be spaced by 2.24 GHz (the $|b\rangle$ state being at higher energy) and the coupling matrix element was taken to be 1 GHz. The rotational constants used, $\frac{1}{2}(B + C)$ and $[A - \frac{1}{2}(B + C)]$, were 0.4119 and 1.7396 GHz for the $|a\rangle$ state; and 0.4116 and 1.7385 GHz for the $|b\rangle$ state. For other details see the text.

the a -type band. The other calculational parameters are included in the figure caption. One can clearly see from the figure that the beat envelope decay rate and its behavior as a function of temperature match our intuitive expectations of this behavior.

To aid direct comparison with experimental data, calculations have also been performed using the 4×4 and 3×3 Hamiltonians which were derived from experimental beat data, and which correspond to the $S_1 + 1420 \text{ cm}^{-1}$ and $S_1 + 1380 \text{ cm}^{-1}$ excitations of anthracene, respectively. These two Hamiltonians appear in the previous paper.⁶ Figure 3 presents calculated decays of the b -type bands of the $S_1 + 1420 \text{ cm}^{-1}$ system for different rotational temperatures. The b -type band was chosen because good experimental data for it are relatively easy to obtain and because the decay is dominated by one beat component (1 GHz with a -1 phase). The rotational constants used for the calculation appear in the figure caption. Sets of other constants yielded qualitatively similar results. The system response function used was 150 ps FWHM (two channels). Clearly, there is a marked rotational temperature effect on the calculated decays. Although all of the decays are modulated similarly at early time, at later times the beats are increasingly washed out as the rotational temperature increases; that is, the apparent decay rate of the beat envelope increases at higher rotational temperatures. Behavior similar to this also occurs in calculated decays of other types of bands in the fluorescence spectrum.

Figures 4 and 5 present calculated decays of the b -type bands in the fluorescence spectrum corresponding to $S_1 + 1380 \text{ cm}^{-1}$ excitation. Such decays⁶ are modulated by beat components at 3.5, 4.9, and 8.4 GHz with phases of $+1$, -1 , and -1 , respectively. The two figures correspond to two different sets of rotational constants. Both

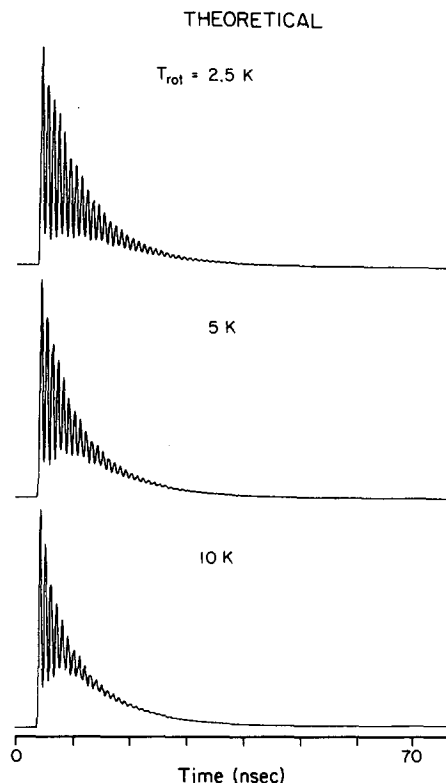


FIG. 3. Simulated b -type decays as a function of rotational temperature for the coupled four-level system described by the Hamiltonian matrix of Eq. (4.6), Ref. 6, which represents the coupling situation at $E_{\text{vib}} = 1420 \text{ cm}^{-1}$ in S_1 anthracene. The randomly generated rotational constants $\frac{1}{2}(B + C)$ and $[A - \frac{1}{2}(B + C)]$ were for the $|a\rangle$, $|b\rangle$, $|c\rangle$, and $|d\rangle$ states, respectively: 0.4119 and 1.7396; 0.4124 and 1.7417; 0.4120 and 1.7401; and 0.4122 and 1.7407 GHz.

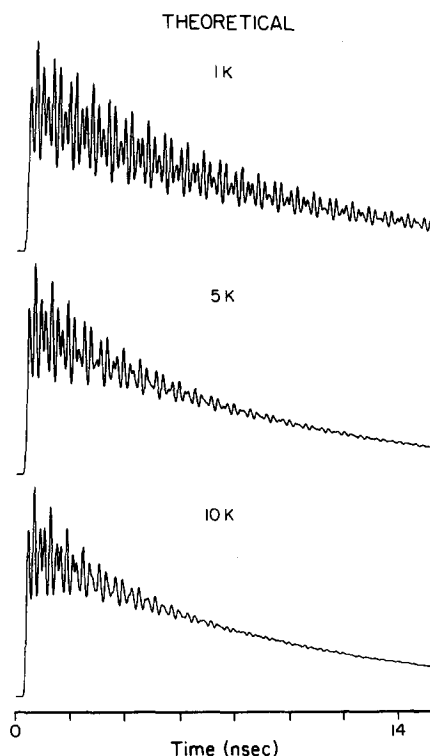


FIG. 4. Simulated b -type decays as a function of rotational temperature for the coupled three-level system described by the Hamiltonian matrix of Eq. (4.3), Ref. 6, which represents the coupling situation at $E_{\text{vib}} = 1380 \text{ cm}^{-1}$ in S_1 anthracene. The rotational constants $\frac{1}{2}(B + C)$ and $[A - \frac{1}{2}(B + C)]$ used were, for the $|a\rangle$, $|b\rangle$, and $|c\rangle$ states, respectively: 0.4127, 1.7428; 0.4119, 1.7395; and 0.4117, 1.7389 GHz.

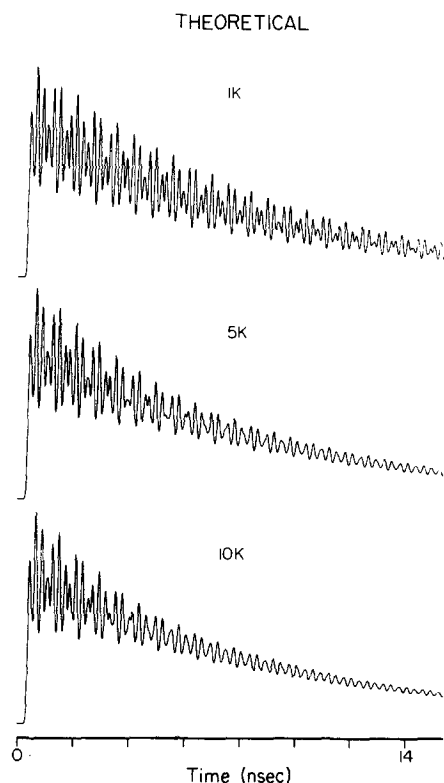


FIG. 5. Same as Fig. 4 but using the rotational constants: 0.4116, 1.7383; 0.4119, 1.7397; and 0.4122, 1.7409 GHz for the $|a\rangle$, $|b\rangle$, and $|c\rangle$ states, respectively.

sets of decays were calculated using a response function of about 90 ps FWHM (six channels). Again, and in both figures, one can see an increase in the beat envelope decay rate as the rotational temperature increases. One may notice an additional point from the decays of Fig. 5. All beat components do not decay at the same rate—one component persists at long time, even for $T_{\text{rot}} = 10$ K. Evidently, those components which turn out to be more (or less) sensitive to rotational temperature are determined by the mismatches in rotational constants. As with the $S_1 + 1420 \text{ cm}^{-1}$ case, calculated decays for the other band types in the $S_1 + 1380 \text{ cm}^{-1}$ spectrum show trends similar to the decays of the b -type band.

III. EXPERIMENTAL

The experimental apparatus and conditions have been reported in the preceding paper.⁶ The dependence of beat parameters on rotational temperature was assessed by measuring fluorescence decays as a function of carrier gas and carrier gas pressure. The carrier gases used were helium, neon, and nitrogen. A small laser-to-nozzle distance (x) dependence was observed for the beat-modulated decays; the greater x , the slower the decay rate of the beat envelope. Because of this, data for different carrier gas parameters are only compared for the same values of x . An excitation wavelength and bandwidth effect was also observed on the decays. In general, decays collected for excitation slightly off of a given band maximum were less modulated than for excitation at a band maximum. Similarly, the greater the bandwidth of excitation, the smaller the observed modulation depths. Again, those

decays collected for different carrier gas parameters are compared herein only if they were measured under identical excitation conditions.

Most data were taken for the $S_1 + 1420 \text{ cm}^{-1}$ excitation in anthracene, although some are presented for the $S_1 + 1380 \text{ cm}^{-1}$ excitation. There are two reasons for the preponderance of $S_1 + 1420 \text{ cm}^{-1}$ data. Firstly, it is relatively easy to measure decays of the intense, spectrally isolated 1750 cm^{-1} band in the $S_1 + 1420 \text{ cm}^{-1}$ fluorescence spectrum.⁶ Secondly, the decays of this band are dominated by one beat component. Thus, they may be fit to functions having a relatively small number of adjustable parameters.

Experimental decays that were dominated by one beat frequency were fit to the convolution of the measured system response function with a function of the form:

$$I(t) = A_1[e^{-\Gamma_1 t} + A_2 e^{-\Gamma_2 t} \cos \omega t] + A_3, \quad (3.1)$$

where ω , A_1 , A_2 , A_3 , Γ_1 , and Γ_2 are parameters. Such fits were accomplished via a nonlinear least squares algorithm.¹⁷ The fit parameters obtained in this way are useful indications of the effects which rotational temperature has on modulation depths (A_2) and quantum beat envelope decay rates (Γ_2).

The Fourier analysis of several experimental decays was also undertaken. The method used is the same as that reported on in the previous paper.⁶ The real parts of the Fourier transforms of entire decays, compensated for response function effects are presented. Unlike in the preceding paper (II), the decays that were subjected to analysis were truncated at a late enough time to substantially eliminate any truncation artifacts in the transforms.

IV. RESULTS

A. $S_1 + 1420 \text{ cm}^{-1}$

Figure 6 presents decays of the 1750 cm^{-1} fluorescence band of anthracene excited to $S_1 + 1420 \text{ cm}^{-1}$ for three different carrier gas conditions. One point which is immediately obvious from the figure is that the amplitude of the 1 GHz component which modulates all three decays, decays at an increasingly faster rate as the carrier gas changes from 75 psig neon to 40 psig helium to 40 psig nitrogen. A more quantitative measure of this trend can be obtained from the fits of these decays. The fit parameters corresponding to the modulation depth of the 1 GHz component are -0.7 , -0.67 , and -0.61 , and the decay rates of the beat envelopes are 0.13, 0.18, and 0.31 GHz for the three decays from top to bottom. While the values for the three modulation depths do not vary very widely and are close to the values previously reported, the values for Γ_2 change from being very close to the unmodulated decay rate (0.11 GHz) to a value which is a factor of ~ 3 greater than this. This trend is matched by the width of the 1 GHz band in the Fourier spectra of the decays of Fig. 6. These spectra, which appear in Fig. 7, show a clear increase in the bandwidth of this component as the carrier gas changes from Ne to He to N_2 .

The changes which occur in Γ_2 as the carrier gas is varied also occur when the carrier gas pressure is varied.

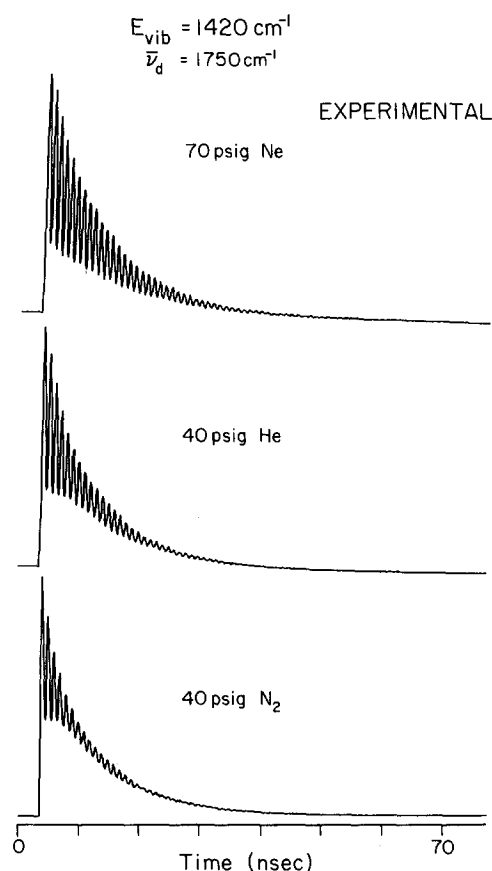


FIG. 6. Measured fluorescence decays of the 1750 cm^{-1} (*b*-type) band in the $E_{\text{vib}} = 1420\text{ cm}^{-1}$ spectrum of jet-cooled anthracene as a function of carrier gas parameters. Decays were measured under identical conditions except for carrier gas. For each decay $x = 6\text{ mm}$, the monochromator resolution $R = 3.2\text{ Å}$, and the laser bandwidth $\text{BW} \approx 2\text{ cm}^{-1}$.

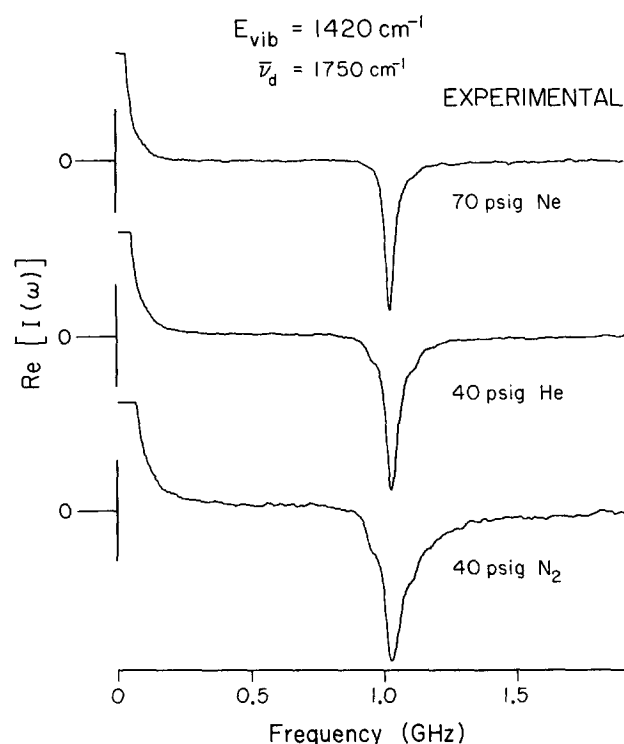


FIG. 7. Fourier spectra $[I(\omega)]$ —see Sec. II B of Ref. 6] of the decays of Fig. 6. The peaks are negative because the 1 GHz component in the decays has a -1 phase.

In general, as the carrier gas pressure increases, Γ_2 decreases. This effect on Γ_2 is not as marked as that which arises when the gas is changed from N_2 to Ne (for instance, a decay taken under the same conditions as for those corresponding to Fig. 6 (top), except that $P = 50\text{ psig}$ rather than 75 psig Ne , was fit to a function with $\Gamma_2 = 0.15\text{ GHz}$) but it is reproducible for all three carrier gases. In the extreme case of *no* carrier gas, the quantum beats are completely washed out, as shown in Fig. 8.

Besides the 1750 cm^{-1} band, the carrier gas dependences of the decays of other fluorescence bands arising from $S_1 + 1420\text{ cm}^{-1}$ excitation have also been measured. In particular, the 390 and 780 cm^{-1} *a*-type fluorescence bands⁶ have been studied. Figure 9 shows results for the 780 cm^{-1} band. The overall beat modulation depth for the decays is less than that of the 1750 cm^{-1} decays for two reasons: (1) the inherent modulation depth for the 1 GHz component is less for the *a*-type bands in the spectrum than for the non-*a*-type 1750 cm^{-1} band and (2) the large detection bandwidth needed to measure decays of the weak 780 cm^{-1} band made it impossible to spectrally isolate the band. The values for Γ_2 derived from fits to the decays of Fig. 9 are in good agreement with those found for the 1750 cm^{-1} decays for similar carrier gas conditions.

B. $S_1 + 1380\text{ cm}^{-1}$

Extensive studies of the effects of carrier gas parameters on the decays of the bands in the $S_1 + 1380\text{ cm}^{-1}$ fluorescence spectrum have not been performed with 80 ps time resolution. Nevertheless, the limited studies which have been performed reveal behavior entirely consistent with that observed for the $S_1 + 1420\text{ cm}^{-1}$ excitation. Figure 10 provides an example. The two decays correspond

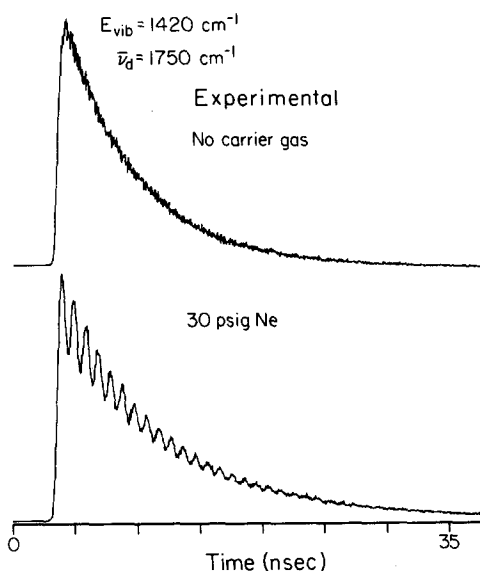


FIG. 8. Measured fluorescence decays for detection of the 1750 cm^{-1} band in the $E_{\text{vib}} = 1420\text{ cm}^{-1}$ spectrum of anthracene for no carrier gas (top) and for 30 psig Ne (bottom), all other conditions being the same ($\text{BW} \approx 3\text{ cm}^{-1}$, $R = 8.0\text{ Å}$, $x = 3\text{ mm}$). The relative lack of modulation in the neon decay compared to the decay of Fig. 6 (top) is primarily due to the poorer detection spectral resolution used in obtaining the former decay.

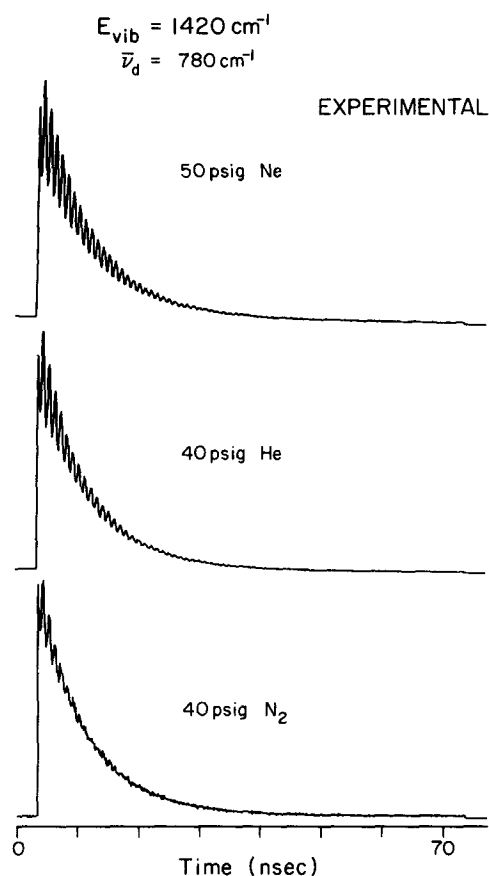


FIG. 9. Measured fluorescence decays for detection of the 780 cm^{-1} (*a*-type) band in the $E_{\text{vib}} = 1420\text{ cm}^{-1}$ spectrum of jet-cooled anthracene as a function of carrier gas parameters. For each decay $x = 3\text{ mm}$, $R = 16\text{ Å}$, and $\text{BW} \approx 2\text{ cm}^{-1}$.

to the detection of the 1460 cm^{-1} (*b*-type) band⁶ in the spectrum for two different carrier gases. Although the presence of three beat frequencies in the decays makes fitting them difficult, it is clear without any fits that the modulations wash out much more quickly in the nitrogen than in the neon decay. Similar behavior has been observed for the 390 (*a*-type) and 1528 cm^{-1} (*c*-type) bands⁶ in the spectrum.

V. DISCUSSION

A. Comparison of simulations with experimental results

It is clear from the simulated decays of Figs. 2–5 that a marked rotational temperature effect on the beat-modulated decays which arise from vibrational states coupled by anharmonic interactions can exist, and that this effect is primarily on the decay rates of quantum beat envelopes. One would now like to directly relate this trend to experimental results.

1. Rotational temperature

The analysis of the experimental results of Sec. IV in terms of the effects of rotational temperature on beats requires some prior knowledge of the way in which different experimental expansion parameters affect the rotational temperature of the sample. Knowledge of this

sort is available from experimental and theoretical sources. Experimentally, we have reported¹¹ the measurement of 0_0^0 *B*-type rotational contours of anthracene for a variety of expansion conditions. The band shape was found to change noticeably with changes in expansion conditions (see Fig. 20, Ref. 11). These changes match the changes that occur in calculated *B*-type contours as a result of variations in the rotational temperature (see Fig. 21, Ref. 11). In particular, the measured contours match the calculated behavior if it is assumed that the rotational temperature follows the trend $T(\text{Ne}) \leq T(\text{He}) < T(\text{N}_2)$ for changes in carrier gas. Estimates of the rotational temperature for various expansion conditions can be made by comparison of the experimental and simulated contours. From our results these estimates go from 1 K for 50 psig Ne to 10 K for 20 psig N_2 . More quantitative fits to experimental contours obtained using better laser resolution have been performed recently.¹⁸ The results are in good agreement with the numbers quoted here.

Theoretically, an idea of the rotational temperature of a free-jet sample can be obtained if it is assumed that the rotational temperature follows the terminal translational temperature of the expansion. Terminal translational temperatures have been calculated¹⁹ for typical expansion conditions used in this laboratory. The general trend and the absolute magnitudes of these temperatures for different carrier gases and pressures are consistent with the conclusions derived from the contour measurements. For example, for a nozzle temperature of 450 K and a pinhole diameter of $150\text{ }\mu\text{m}$, 40 psig expansions of Ne, He, and N_2 were calculated to have terminal translational temperatures of 0.9, 1.2, and 3.9 K, respectively. One expects the rotational temperatures of such expansions seeded with anthracene to be somewhat higher than these

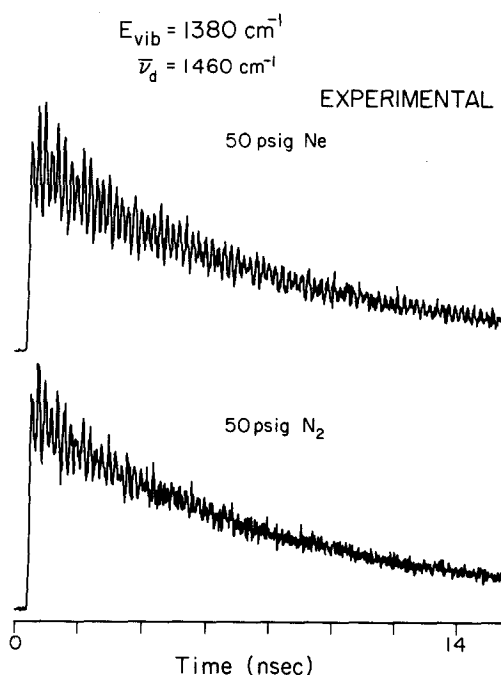


FIG. 10. Measured fluorescence decays for detection of the 1460 cm^{-1} (*b*-type) band in the $E_{\text{vib}} = 1380\text{ cm}^{-1}$ spectrum of anthracene as a function of carrier gas parameters. For each decay $x = 3\text{ mm}$, $R = 0.8\text{ Å}$, and $\text{BW} \approx 2\text{ cm}^{-1}$.

values, being that rotational degrees of freedom do not cool as efficiently as translational degrees of freedom.

2. Effect of rotational temperature on measured decays

Having established a semiquantitative link between expansion parameters and rotational temperature, one can now consider the changes in quantum beat decays with rotational temperature. As was noted in Sec. IV, the major trend which emerges from the experimental results is that the decay rate of quantum beat envelopes increases as the carrier gas is changed from Ne to He to N₂. Interpreting this trend strictly in terms of the changes induced in rotational temperature with changes in carrier gas, one may say that as the rotational temperature increases, the beat decay rate increases, as well. Now, it may be argued that some carrier gas dependent collisional interaction between the carrier gas and anthracene is responsible for the observed trend, instead of changes in rotational temperature. However, if this were the case, the beat decay rate would be expected to increase as the pressure of a given carrier gas were increased. This is the opposite of what is observed. On the other hand, this kind of behavior with pressure is consistent with rotational temperature changes since the temperature would be expected to decrease with increasing pressure.¹⁹ Therefore, one arrives at the conclusion that increasing the rotational temperature of anthracene increases the quantum beat decay rates of the fluorescence decays corresponding to the $S_1 + 1380\text{ cm}^{-1}$ and $S_1 + 1420\text{ cm}^{-1}$ excitations. Complementary to this effect of rotational temperature on decay parameters is the effect of temperature on the widths of the beat component in the Fourier spectra (Fig. 7). Just as one might expect, the increase in beat decay rate with increasing rotational temperature is directly linked to an increase in bandwidth in the frequency domain.

3. Simulations and coupling parameters

The changes with rotational temperature that occur in measured decays are quite similar to those changes which occur in simulated decays calculated assuming anharmonic coupling and rotational constant mismatches. This similarity is readily seen in a comparison of Figs. 3 and 6, and Figs. 4 and 10 (note the very close matches between simulated decays at various temperatures and measured decays for different carrier gas parameters).

We take these close similarities as strong evidence that the observed beat envelope decay behavior arises from some anharmonic coupling-rotational constant mismatch mechanism. The operation of such a mechanism in enhancing beat decay rates is perhaps best explained by reference to what happens in the frequency domain. Given small variations with rotational level in the Hamiltonian matrices [$H_0(J, K_a)$] describing the coupling of a set of rovibrational levels, one expects similar variations in the eigenvalues of these matrices. Given also a situation wherein $H_0(J, K_a)$ tends to deviate more from $H_0(J', K'_a)$ when J and K_a differ more from J' and K'_a [cf. Eq. (2.4)], then one expects the eigenvalues of the two matrices to

differ more for more widely separated J, K_a and J', K'_a . Now at low rotational temperatures, there is a narrow distribution of populated rotational levels. Thus, the relevant values of J, K_a are all close to one another and the variations in eigenvalues of the relevant $H_0(J, K_a)$ are small. As T increases, however, more widely varying values of J, K_a become relevant, and the variations in eigenvalues increase. Small variations in eigenvalues translate directly into beat frequency bandwidths. Thus, it is clear that these beat frequency bandwidths will increase with increasing rotational temperature given the hypotheses about $H_0(J, K_a)$. Moreover, since the rate of decay of a beat component can be directly related to the bandwidth of that component, it is also clear that beat decay rates should increase with increasing rotational temperature.

Note that in the preceding paragraph we have emphasized the smallness of the variations in $H_0(J, K_a)$. Large variations do not, in general, give rise to the sort of quasicontinuous variations in eigenvalues which result in bandwidths for beat components. It is the smallness of the variations in $H_0(J, K_a)$ that would be expected given anharmonic coupling and rotational constant mismatch that renders such a mechanism a plausible explanation for the observed behavior.

A connection between beat envelope decay rates and the rotational constants of zero-order vibrational states could turn out to have very useful consequences in the study of intramolecular vibrational energy redistribution (IVR). Because different classes of vibrational motions in a molecule would be expected to have rotational constants with characteristically different deviations from average values, then knowledge of these deviations could facilitate the assignment of vibrational states in terms of the normal modes of the molecule. The ability to do this for the coupled vibrational states giving rise to an IVR process is of tremendous and obvious value to the full understanding of the process. To help accomplish this with beat envelope decay rates, one would require a more quantitative theoretical connection between these rates and rotational constant mismatches. Experimentally, more precise measurements of rotational temperatures and decay rates (especially for decays modulated by a number of components) would be needed. Such advances are certainly not inconceivable and, indeed, may be at hand.

4. Coriolis interactions

At this point, a few remarks concerning the uniqueness of the anharmonic coupling-rotational constant mismatch mechanism in explaining the trend of the experimental results should be made. One can certainly envision other coupling mechanisms which would give rise to distributions of beat frequencies dependent on rotational temperature. In particular, one might consider Coriolis coupling.^{9,20} Coriolis coupling, however, has matrix elements which are steeply dependent on J, K_a . Given a Hamiltonian matrix with off-diagonal elements solely determined by Coriolis coupling, one would not expect the simple beat patterns and small numbers of beat components observed in the experimental decays.⁶ Indeed,

even decay simulations done by us using a 2×2 Hamiltonian matrix have been found to produce extremely complicated beat patterns. Nevertheless, this is not proof positive that Coriolis coupling does not bear any influence on the experimental results. We say this because Hamiltonian matrices with interaction matrix elements solely determined by Coriolis coupling are not the only ones in which such coupling may be realized. In fact, it is more probable that most real Hamiltonians consist of some states coupled anharmonically and other ones coupled (probably weakly) by Coriolis interactions. This kind of situation could give rise to subtle rotational temperature effects such as have been reported on herein. And, they may explain other, less subtle effects reported on elsewhere.⁵ The large number of possibilities for such mixed coupling has precluded, however, any detailed consideration here.

Manifestations of Coriolis interactions in the spectra and decay behavior of polyatomics such as benzene,²¹ pyrazine,²² and formaldehyde¹⁶ have been reported. Given the apparent importance of Coriolis couplings in these cases, it is pertinent to compare them with the case of IVR in anthracene. For the above-mentioned molecules, we would note several differences from the anthracene situation: (a) interelectronic state coupling is involved (or thought to be involved) in the former cases, (b) the rotational constants are larger for these smaller molecules, which leads to larger Coriolis coupling constants,^{15,20} and (c) these other cases involve significantly larger amounts of vibrational energy than the energies corresponding to our anthracene results. It is possible that the apparent dominance of anharmonic interactions over Coriolis coupling in the case of IVR in anthracene, as opposed to that which obtains for the other cases, is due to one or more of the differences given above. To further substantiate and generalize this requires more experimental work to obtain high resolution spectra and time-resolved results on the same molecules.

B. Rotational dephasing

The theoretical and experimental results of this paper on the role of rotations in IVR can be related to temperature effects on intramolecular dephasing. At 0 K rotational temperature, IVR occurs with the rotational "bath" being essentially empty. Γ_2 approaches the fluorescence decay rate Γ_1 in this limit. Or, in the language of the density matrix formalism, T_2 approaches T_1 . As the rotational temperature increases, however, rotational dephasing, brought about by the many overlapping incoherent excitations from thermally populated J , K_a levels, is possible. This pure dephasing causes T_2 to become less than T_1 . In a sense, the rotational reservoir in this case is similar to the phonon reservoir in solids, for which T_2 has been measured to be less than T_1 at temperatures above ~ 2 K.²³

VI. CONCLUSIONS

We have considered theoretically the effects which the rotational level structure can have on beat-modulated fluorescence decays that arise from anharmonically coupled vibrational states. For small mismatches in rotational

constants between coupled vibrational states, these effects primarily take the form of increased decay rates for quantum beat envelopes relative to the overall fluorescence decay rates. Experimental results of decays as a function of carrier gas parameters reveal behavior in anthracene which is entirely consistent with the theoretical results. Taken together, all the results argue convincingly that (1) vibrational coherence effects need not be washed out by the rotational level structure, (2) anharmonic coupling is the primary coupling interaction giving rise to phase-shifted beats in anthracene at the reported excess energies, and (3) the effects of rotations on IVR can be assessed by time-resolved experiments.

ACKNOWLEDGMENT

This work was supported by the National Science Foundation through Grant No. DMR-8105034.

- ¹ P. M. Felker and A. H. Zewail, *J. Chem. Phys.* **82**, 2961 (1985).
- ² P. M. Felker and A. H. Zewail, *Chem. Phys. Lett.* **102**, 113 (1983).
- ³ P. M. Felker and A. H. Zewail, *Phys. Rev. Lett.* **53**, 501 (1984).
- ⁴ P. M. Felker and A. H. Zewail, *Chem. Phys. Lett.* **108**, 303 (1984).
- ⁵ W. R. Lambert, P. M. Felker, and A. H. Zewail, *J. Chem. Phys.* **81**, 2217 (1984).
- ⁶ P. M. Felker and A. H. Zewail, *J. Chem. Phys.* **82**, 2975 (1985).
- ⁷ (a) See, for example, the discussion given by R. E. Smalley, *Annu. Rev. Phys. Chem.* **34**, 129 (1983); (b) See also K. Freed and A. Nitzan, *J. Chem. Phys.* **73**, 4765 (1980).
- ⁸ Experimentally, the justification derives from the fact that no quantum beats have been observed for a large number of low energy ($E_{\text{vib}} < 1200 \text{ cm}^{-1}$) excitation bands in anthracene. Given observable coherence effects involving rotational levels in the same vibrational manifold, one would expect to observe beats for excitation of essentially every band. Theoretically, one notes selection rules which limit both the number of levels which can be prepared coherently via excitation and which restrict the number of beating fluorescence transitions from these coherently prepared levels. Further, one notes the large distribution of beat frequencies and the large number of high frequency components to be expected from the coherent preparation of rotational levels within the same vibrational state.
- ⁹ See G. Herzberg, *Infrared and Raman Spectra of Polyatomic Molecules* (Van Nostrand, Princeton, 1945).
- ¹⁰ See Sec. II of Ref. 1 (paper I). Note that $I_r(J, K_a, t)$ used herein corresponds to $I_r(t)$ in Ref. 1 in the sense that both are associated with a single $N \times N$ Hamiltonian matrix. $I_r(t)$ in this paper, however, is associated with the large number of independent matrices describing the vibrational coupling interactions as a function of rotational level.
- ¹¹ W. R. Lambert, P. M. Felker, J. A. Syage, and A. H. Zewail, *J. Chem. Phys.* **81**, 2195 (1984).
- ¹² E. B. Wilson, *J. Chem. Phys.* **3**, 276 (1935).
- ¹³ S. M. Beck, M. G. Liverman, D. M. Monts, and R. E. Smalley, *J. Chem. Phys.* **70**, 232 (1979).
- ¹⁴ W. E. Howard and E. W. Schlag, in *Radiationless Transitions*, edited by S. H. Lin (Academic, New York, 1980), p. 81.
- ¹⁵ F. A. Novak, S. A. Rice, M. D. Morse, and K. F. Freed, Ref. 14, p. 135.
- ¹⁶ E. K. C. Lee and G. L. Loper, Ref. 14, p. 1, and references therein.
- ¹⁷ P. R. Bevington, *Data Reduction and Error Analysis for the Physical Sciences* (McGraw-Hill, New York, 1969).
- ¹⁸ B. W. Keelan and A. H. Zewail, *J. Chem. Phys.* **82**, 3011 (1985).
- ¹⁹ W. R. Lambert, Ph.D. thesis, California Institute of Technology, 1982.
- ²⁰ E. B. Wilson, *J. Chem. Phys.* **4**, 313 (1936).
- ²¹ E. Riedle, H. J. Neusser, and E. W. Schlag, *J. Phys. Chem.* **86**, 4847 (1982).
- ²² D. B. McDonald, G. R. Fleming, and S. A. Rice, *Chem. Phys.* **60**, 335 (1981).
- ²³ M. J. Burns, W.-K. Liu, and A. H. Zewail, in *Spectroscopy and Excitation Dynamics of Condensed Molecular Systems, Vol. 4*, edited by V. M. Agranovich and R. M. Hochstrasser (North-Holland, Amsterdam, 1983), p. 301.